AD_____

Award Number: DAMD17-99-1-9130

TITLE: Finite Element Based Photon Migration Imaging

PRINCIPAL INVESTIGATOR: Huabei Jiang, Ph.D.

CONTRACTING ORGANIZATION: Clemson University
Clemson, South Carolina 29634-5702

REPORT DATE: May 2003

TYPE OF REPORT: Annual Summary

PREPARED FOR: U.S. Army Medical Research and Materiel Command
Fort Detrick, Maryland 21702-5012

DISTRIBUTION STATEMENT: Approved for Public Release;
Distribution Unlimited

The views, opinions and/or findings contained in this report are those of the author(s) and should not be construed as an official Department of the Army position, policy or decision unless so designated by other documentation.

20030902 122

REPORT DOCUMENTATION PAGE

Form Approved
OMB No. 074-0188

Public reporting burden for this collection of information is estimated to average 1 hour per response, including the time for reviewing instructions, searching existing data sources, gathering and maintaining the data needed, and completing and reviewing this collection of information. Send comments regarding this burden estimate or any other aspect of this collection of information, including suggestions for reducing this burden to Washington Headquarters Services, Directorate for Information Operations and Reports, 1215 Jefferson Davis Highway, Suite 1204, Arlington, VA 22202-4302, and to the Office of Management and Budget, Paperwork Reduction Project (0704-0188), Washington, DC 20503

1. AGENCY USE ONLY (Leave blank)	2. REPORT DATE	3. REPORT TYPE AND DATES COVERED
	May 2003	Annual Summary (1 May 02 - 30 Apr 03)

4. TITLE AND SUBTITLE
Finite Element Based Photon Migration Imaging

5. FUNDING NUMBERS
DAMD17-99-1-9130

6. AUTHOR(S)
Huabei Jiang, Ph.D.

7. PERFORMING ORGANIZATION NAME(S) AND ADDRESS(ES)
Clemson University
Clemson, South Carolina 29634-5702

E-MAIL:
HJIANG@clemson.edu

8. PERFORMING ORGANIZATION REPORT NUMBER

9. SPONSORING / MONITORING AGENCY NAME(S) AND ADDRESS(ES)
U.S. Army Medical Research and Materiel Command
Fort Detrick, Maryland 21702-5012

10. SPONSORING / MONITORING AGENCY REPORT NUMBER

11. SUPPLEMENTARY NOTES

12a. DISTRIBUTION / AVAILABILITY STATEMENT
Approved for Public Release; Distribution Unlimited

12b. DISTRIBUTION CODE

13. ABSTRACT (Maximum 200 Words)

This research is aimed at developing a new optical approach, called "Photon Migration Imaging", for breast cancer detection and diagnosis. The project will develop computer software and conduct phantom experiments to achieve the proposed goals. During the third year of this project, we have implemented and evaluated the 2D image enhancing schemes especially in the areas of dual meshing and total variation. We have also started to implement the 3D reconstruction algorithms based on these enhancing schemes. We have conducted considerable simulation and phantom experiments for optical and fluorescence lifetime imaging. The successful experiments have confirmed the imaging capability of our reconstruction software.

14. SUBJECT TERMS	15. NUMBER OF PAGES
breast cancer, photon migration imaging	12
	16. PRICE CODE

17. SECURITY CLASSIFICATION OF REPORT	18. SECURITY CLASSIFICATION OF THIS PAGE	19. SECURITY CLASSIFICATION OF ABSTRACT	20. LIMITATION OF ABSTRACT
Unclassified	Unclassified	Unclassified	Unlimited

Table of Contents

Introduction

The ability of near-infrared (NIR) light-based techniques to noninvasively image and analyze tissue structure and function promises their great potential for detection and diagnosis of breast cancer. Optical diagnostic techniques allow us to not only enhance the existing capabilities, but to eliminate the need for physical biopsies. In addition, optical imaging is inexpensive and portable, which indicates that optical imaging could be an ideal candidate for routine breast screening. However, since the scattering properties of tissues convolute re-emitted NIR signals, the extraction of pertinent information continues to remain elusive. An understanding of light propagation and light-tissue interaction is required before the optical technologies can substantially impact diagnostic medicine.

Research efforts in the Biomedical Optics Laboratory at Clemson University are focused on the biophysics of light propagation and light-tissue interaction in order to engineer appropriate approaches for noninvasive breast imaging and spectroscopy. Specifically, we are developing indirect optical/fluorescence approaches using photon migration measurements in the continuous-wave and frequency domains. These indirect optical/fluorescence approaches or image reconstructions are computationally based on the powerful finite element methods. A CCD-based optical spectroscopic imaging system is already operational in our laboratory for continuous-wave tomographic photon migration measurements, while a frequency-domain system has also been constructed. Using these optical systems coupled with our finite element based reconstruction algorithms, we will be able to extract spatial/spectroscopic maps of tissue optical properties, lifetime and/or yield of endogenous and exogenous fluorescent probes. Since metabolic tissue states can be identified by our approaches, diagnostic information is also obtained in addition to detection of tumor.

This Career Development application for support of Dr. Huabei Jiang will facilitate the establishment/continuation of these research activities. Interdisciplinary interactions with the Greenville Hospital System (Greenville, SC) will be enhanced, which insures the direction of research towards a clinically pertinent and feasible system.

Body

This report describes work accomplished during the fourth year of a proposed four-year study (with one-year no-cost extension). This Career Award supports Dr. Jiang's research on optical and fluorescence imaging using both continuous-wave and frequency-domain measurements. The focus of the proposed work in Year 4 is the implementation and evaluation of image enhancing schemes in the areas of dual meshing and total variation; continued phantom studies of image reconstructions with dye-free or dye-laden phantom background; continued implementation of 3D reconstruction algorithms.

Software work: We have implemented and evaluated important image enhancing schemes in the areas of dual meshing and total variation. Extensive simulation and phantom experiments have been conducted to complete these software developments. We have also started to implement the 3D reconstruction algorithms based on these image enhancing schemes.

Phantom Experiments: Using our frequency-domain imaging system, we have conducted extensive phantom experiments for both optical and fluorescence reconstruction with dye-free background and dye-laden background. Our experimental setup used was the automated multi-channel frequency-domain system mentioned above. The system employed a radio-frequency intensity-modulated near-infrared beam. The laser beam was sent to the phantom by 16 fiber optic bundles coupled with a high precision moving stage. The diffused radiation was received by another 16 channel fiber optic bundles and delivered to a thermo-electric cooled PMT. A second PMT was used to record the reference signal. These PMTs were supplied at a radio-frequency modulated current with 0.1-1KHz shift. The intermediary frequency signal obtained from the PMTs was processed using a National Instruments board. For every source position, 16 measurements for each detector were made, taking alternatively 100 ms samples for sample and reference signals. Fluorescence signals were obtained through an 830nm or 690nm interference filter placed in front of the detection PMT. dc, ac intensity and phase shift between reference and sample signals were obtained using FFT Labview routines. The total data collection time for 256 measurements was 8 minutes.

Solid phantom was used to mimic the human tissue. It was made of agar, Intralipid, black ink and fluorescent dyes. The absorption and the reduced scattering coefficients are linear with the ink and Intralipid concentrations, respectively. While ICG and DTTCI dyes were continually used in these experiments, we have also used oxygen-sensitive dyes including Sn(IV)Chlorin-e_6-Cl_2-3Na (SCCN). Agar was used to make the phantom solid. The absorption and fluorescent emission peaks of this oxygen-sensitive dye is about 660 nm and 690nm, respectively. The solid phantom consisted of a cylindrical background and a cylindrical heterogeneity. These experiments show that we may be able to obtain the tissue oxygen concentration images by the use of oxygen-sensitive dyes. This could provide optical imaging a unique capability to distinguish between benign and malignant breast tumors because the oxygen concentration in these two types of tumors often is distinct. Some of the image results have been published in a peer-reviewed journal (see the manuscript provided in the *Appendix* to this Summary Report).

Key Research Accomplishments

1. We have implemented and evaluated the 2D image enhancing schemes especially in the areas of dual meshing and total variation. We have also started to implement the 3D reconstruction algorithms based on these image enhancing schemes.
2. We have conducted considerable phantom experiments for optical and fluorescence lifetime imaging. The successful experiments have confirmed the imaging capability of our reconstruction software.

Reportable Outcomes (see the Appendix to this Summary Report)

Conclusions

We have made a significant progress that has fulfilled most of the statement of work proposed for Year 4 of this project. We believe that we will be able to fulfil or exceed the work statement for Year 4 within the extended year.

Appendix

E. Shives, Y. Xu, and H. Jiang, "Fluorescence lifetime tomography of turbid media based on an oxygen-sensitive dye," *Opt. Express* **10**, 1557-1562 (2002).

Fluorescence lifetime tomography of turbid media based on an oxygen-sensitive dye

Eric Shives, Yong Xu, and Huabei Jiang
Department of Physics & Astronomy, Clemson University, Clemson, SC 29634
hjiang@clemson.edu

http://virtual.clemson.edu/groups/bmol

Abstract: We present for the first time experimental images of fluorescence lifetime distribution using model-based reconstruction. The lifetime distribution in our phantom experiments was realized through using an oxygen-sensitive dye [Sn(IV)Chlorin-e_6-Cl_2-3Na (SCCN)] whose lifetime varied with the oxygen concentration provided in the target and background media. The fluorescence tomographic data was obtained using our multi-channel frequency-domain system. Spatial maps of fluorescence lifetime were achieved with a finite element based reconstruction algorithm.

©2002 Optical Society of America

OCIS codes: (110.6960) Tomography; (170.3010) Image reconstruction techniques; (170.3650) Lifetime-based sensing; (170.6280) Spectroscopy, fluorescence and luminescence

References and links

1. M. A. O'Leary, D. A. Boas, X. D. Li, B. Chance, and A. G. Yodh, "Fluorescence lifetime imaging in turbid media," Opt. Lett. **21**, 158-160 (1996).
2. J. Chang, H.L. Graber, R.L. Barbour, "Luminescence optical tomography of dense scattering media," JOSA A **14**, 288-299(1997).
3. D. Y. Paithankar, A.U. Chen, B. W. Pogue, M. S. Patterson, and E. M. Sevick-Muraca, "Imaging of fluorescent yield and lifetime from multiply scattered light reemitted from random media," Appl. Opt. **36**, 2260-2272 (1997).
4. H. Jiang, "Frequency-domain fluorescent diffusion tomography: a finite-element-based algorithm and simulations," Appl. Opt. **37**, 5337-5343 (1998).
5. R. Richards-Kortum, E. Sevick-Muraca, "Quantitative optical spectroscopy for tissue diagnosis," Annu. Rev. Phys. Chem. **47**, 555-606 (1996).
6. J. Reynolds, T. Troy, R. Mayer, A. Thompson, D. Waters, J. Cornell, P. Snyder, E. Sevick-Muraca, "Imaging of spontaneous canine mammary tumors using fluorescent contrast agents," Photochem. Photobiol. **70**, 87-94(1999).
7. V. Ntziachristos, A. Yodh, M. Schnall, B. Chance, "Concurrent MRI and diffuse optical tomography of breast after indocyanine green enhancement," PNAS **97**, 2767-2772(2000).
8. P. Hohenberger, C. Felgner, W. Haensch, and P. M. Schlag "Tumor oxygenation correlates with molecular growth determinants in breast cancer," Breast Cancer Research and Treatment **48**, 97-106 (1998).
9. E. R. Carraway, J. N. Demas, B. A. DeGraff, and J. R. Bacon, "Photophysics and photochemistry of oxygen sensors based on luminescent transition-metal complexes," Analytical Chemistry **63**, 337-342 (1991).
10. D. B. Papkovsky, G. V. Ponomarev, W. Trettnak, and P. O'Leary, "Phosphorescent complexes of porphyrin ketones: Optical properties and applications to oxygen sensors," Analytical Chemistry **67**, 4112-4117 (1995).
11. S. A. Vinogradov, L. Lo, W. T. Jenkins, S. M. Evans, C. Koch, and D. F. Wilson, "Noninvasive imaging of the distribution of oxygen in tissue *in vivo* using near-infrared phosphors," Biophysical Journal **70**, 1609-1617 (1996).
12. F. N. Castellano and J. R. Lakowicz, "A water-soluble luminescence oxygen sensor," Photochemistry and Photobiology **67**, 179-183 (1998).
13. J. R. Lakowicz, Principles of Fluorescence Spectroscopy, Plenum Press, New York (1983).
14. V. Ntziachristos, R. Weissleder, "Experimental three-dimensional fluorescence reconstruction of diffuse media by use of a normalized Born approximation," Opt. Lett. **26**, 893-895(2001).
15. M. Eppstein, D. Hawrysz, A. Godavarty, E. Sevick-Muraca, "Three-dimensional, Bayesian image reconstruction from sparse and noisy data sets: Near-infrared fluorescence tomography," PNAS **99**, 9619-9624 (2002).

#1668 - $15.00 US
Received September 17, 2002; Revised December 18, 2002
(C) 2002 OSA

16. X. D. Li, M. A. O'Leary, D. A. Boas, B. Chance, and A. G. Yodh, "Fluorescent diffuse photon density waves in homogeneous and heterogeneous turbid media: analytic solutions and applications," Appl. Opt. **35**, 3746-3758 (1996).
17. N. Iftimia and H. Jiang, "Quantitative optical image reconstruction of turbid media by use of direct-current measurements," Appl. Opt. **39**, 5256-5261 (2000).
18. Y. Yang, N. Iftimia, Y. Xu, and H. Jiang, "Frequency-domain fluorescent diffusion tomogrphy of turbid media and in vivo tissues," SPIE **4250**, 537-545 (2001).
19. D. Elson , S. Webb, J. Siegel, K. Suhling, D. Davis, J. Lever, D. Phillips, A. Wallace, and P. French, "Biomedical applications of fluorescence lifetime imaging," Opt. Photonics News **13**, 27-32 (November 2002).

1. Introduction

Recently the idea of reconstruction-based fluorescence diffusion tomography has been developed for clinical applications such as breast cancer detection and tissue functional mapping [1-4]. This new imaging approach relies on the fact that the lifetime of fluorophores in tissue can potentially provide tissue functional information such as tissue oxygenation, pH, and enzyme [2-5]. It is also based on the fact that the fluorophores may preferentially accumulate in tumors, hence providing enhanced sensitivity for cancer detection [6,7]. In this type of indirect imaging method, a model-based reconstruction algorithm is crucial which allows for the formation of a spatial map of fluorophore concentration and/or lifetime in tissue.

This paper explores the possibility of fluorescence lifetime tomography (FLT) based on oxygen-sensitive dyes. Hohenberger *et al.* [8] have recently shown that the oxygen concentration for healthy and cancerous breast tissue is significantly different. They reported the values of oxygen concentration for healthy, fibroadenomas (benign lesions) and malignant lesions as 56, 63 and 44 mmHg, respectively. Fibroadenomas have higher oxygen content than the surrounding tissue because the solubility for oxygen of the fluid inside is presumably higher. Conversely, a malignant tumor has lower oxygen content than the surrounding tissue because of the high rate of mitosis. Mitosis requires a lot of energy from the cell that raises the cells metabolic rate. As the metabolic rate of the cell increases, oxygen use goes up and therefore the oxygen content in the malignant tumor is less than the surrounding tissue. It has also been shown in the literature [9-12] that the lifetimes of some fluorescent dyes are sensitive to the amount of oxygen present in solution/tissue. The more oxygen there is, the lower the lifetime: oxygen concentration and lifetime is quantitatively correlated by the well-known Stern-Volmer equation [13]. Thus tissue oxygen concentration maps can be derived from lifetime images obtained using FLT.

To date fluorescence reconstructions are largely limited to imaging of fluorophore concentration [14], or fluorescence-enhanced absorption [15]. In this paper we present successful quantitative reconstruction of lifetime distributions from frequency-domain measurements using tissue-like phantoms containing SCCN dye with varied oxygen content in the target and background. To the best of our knowledge, the results shown here are the first experimentally reconstructed images for which recovery of lifetime profile has been achieved with absolute ac excitation and fluorescent emission data.

2. Methods and Materials

2.1. Reconstruction Algorithm

Based on a set of coupled diffusion equations that describe the propagation of both excitation and fluorescent emission light in tissues, our reconstruction approach casts image formation as a nonlinear optimization problem in which the optimization parameters are optical and fluorescent properties. While the details of our reconstruction algorithm can be found in Ref. 4, we outline a special formulation for the phantom study reported here. In frequency-domain, it is known that propagation of both excitation and fluorescent emission light in tissues can be described by the following coupled diffusion equations [3,16]:

#1668 - $15.00 US
Received September 17, 2002; Revised December 18, 2002
(C) 2002 OSA

$$\nabla\cdot[D_x(r)\nabla\Phi_x(r,\omega)]-\left[\mu_{a_x}(r)-\frac{i\omega}{c}\right]\Phi_x(r,\omega)=-S(r,\omega) \quad (1)$$

$$\nabla\cdot[D_m(r)\nabla\Phi_m(r,\omega)]-\left[\mu_{a_m}(r)-\frac{i\omega}{c}\right]\Phi_m(r,\omega)=-\eta(r)\mu_{a_{x\to m}}\Phi_x(r,\omega)\frac{1+i\omega\tau(r)}{1+\omega^2\tau(r)^2} \quad (2)$$

where $\Phi_{x,m}$ is the photon density for excitation (subscript x) or fluorescent light (subscript m), $D_{x,m}$ is the diffusion coefficient, $\mu_{a_{x,m}}$ is the absorption coefficient due to contributions from both non-fluorescing chromophores and fluorescent dye, $\mu_{a_{x\to m}}$ is the absorption coefficient for the excitation light due to contribution from fluorescent dye, ω is the modulation frequency, c is the velocity of light in the medium, and η and τ are the fluorescent quantum yield and lifetime, respectively. $S(r,\omega)$ is the excitation source term in (1) which for a point source can be written as $S=S_0\delta(r-r_0)$, where S_0 is the source strength and $\delta(r-r_0)$ is the Dirac-delta function for a source at r_0. The diffusion coefficient can be written as $D_{x,m}(r)=1/3[\mu_{a_{x,m}}(r)+\mu'_{s_{x,m}}(r)]$ where $\mu'_{s_{x,m}}(r)$ is the reduced scattering coefficient. In this study we use the non-zero photon density boundary conditions (BCs) or Type III BCs: $-D_{x,m}\nabla\Phi_{x,m}\cdot\hat{n}=\alpha\Phi_{x,m}$, where $\hat{n}$ is the unit normal vector for the boundary surface and α is a coefficient that is related to the internal reflection at the boundary.

Making use of finite element discretizations, we can obtain two matrix equations for Eqs. (1) and (2) and realize other derived matrix relations through differentiation, which lead to a set of equations capable of inverse problem solution:

$$[A_{x,m}]\{\Phi_{x,m}\}=\{b_{x,m}\} \quad (3)$$

$$[A_{x,m}]\{\partial\Phi_{x,m}/\partial\chi\}=\{\partial b_{x,m}/\partial\chi\}-[\partial A_{x,m}/\partial\chi]\{\Phi_{x,m}\} \quad (4)$$

$$\left(\Im_{x,m}^T\Im_{x,m}+\lambda I\right)\Delta\chi=\Im_{x,m}^T(\Phi_{x,m}^o-\Phi_{x,m}^c) \quad (5)$$

where the elements of matrix $[A_{x,m}]$ are $(a_{x,m})_{ij}=<-D_{x,m}\nabla\psi_j\cdot\nabla\psi_i-(\mu_{a_{x,m}}-\frac{i\omega}{c})\psi_j\psi_i>$ where $<\ >$ indicates integration over the problem domain; ψ_i and ψ_j are locally spatially-varying Lagrangian basis functions; the entries in column vectors $\{b_{x,m}\}$ are $(b_x)_i=-\langle S\psi_i\rangle+\alpha\sum_{j=1}^{M}(\Phi_x)_j\oint\psi_j\psi_i ds$ and $(b_m)_i=-<\eta\mu_{a_{x\to m}}\sum_{j=1}^{N}(\Phi_x)_j\psi_j\psi_i\frac{1-i\omega\tau}{1+\omega^2\tau^2}>+\alpha\sum_{j=1}^{M}(\Phi_m)_j\oint\psi_j\psi_i ds$ where $\oint$ expresses integration over the boundary surface where Type III BCs have been applied. χ expresses D_x, μ_{a_x}, $\eta\mu_{a_{x\to m}}$, or τ; $\Im_{x,m}$ is the Jacobian matrix that should be formed

#1668 - $15.00 US
Received September 17, 2002; Revised December 18, 2002
(C) 2002 OSA

from $\partial\Phi_{x,m}/\partial\chi$ at the boundary measurement sites; $\Delta\chi$ is the update vectors for the optical and fluorescent property profiles; I is the identity matrix; λ may be a scalar or a diagonal matrix; and $\Phi^{o,c}_{x,m} = \{(\Phi^{o,c}_{x,m})_1, (\Phi^{o,c}_{x,m})_2, \cdots (\Phi^{o,c}_{x,m})_N\}^T$ and $(\Phi^{o}_{x,m})_i$ and $(\Phi^{c}_{x,m})_i$, respectively, are observed and calculated photon density for i=1, 2, ..., M boundary locations. Note that to estimate D_x, μ_{a_x}, $\eta\mu_{a_{x\to m}}$, and τ spatially we expand these quantities in a similar fashion to Φ as a finite sum of unknown coefficients multiplied by the locally defined Lagrangian basis functions. In FLT, images are formed by iteratively solving Eqs. (3)-(5) and updating the optical and fluorescent property distributions from presumably uniform initial estimates of these properties.

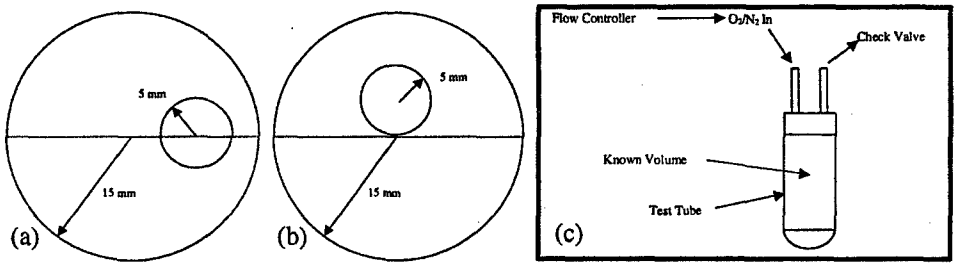

Fig. 1. (a) and (b) Experimental geometries under study, with an off-centered target 7mm away from the boundary (a) and an off-centered target 9 mm away from the boundary (b). (c) Gas delivery system.

2.2. Experiments

Our experimental setup is an automated multi-channel frequency-domain imaging system that has been described in detail elsewhere [17,18]. In this system, an intensity-modulated 635-nm light from a 30 mW diode laser (Thorlabs) is sequentially sent to the phantom by sixteen 1-mm fiber optic bundles. For each source position, the diffused light is received at sixteen detector positions along the surface of the cylindrical phantom and sequentially delivered to a photomultiplier tube (PMT) (Hamamatsu R928). A second PMT is used to record the reference signal (<5% of the modulated light from the diode laser). The two PMTs are supplied by the radio-frequency (RF) generators (IFR Americas 2032A) at a modulated current of 100 MHz with 1.0 KHz shift. Both source and detector fiber bundles are firmly held by a black-painted metal ring structure. The multiplexing of the source/detector fibers are accomplished by two moving stages (Melles-Griot). dc, ac and phase shift signals are obtained using the standard heterodyne technique controlled by Fast Fourier Transform (FFT) Labview routines. Fluorescence signals are obtained through an 700 ± 10 nm interference filter placed in front of the detection PMT. For each experimental configuration, a total of 3x256 measurements (256 dc, ac and phases each) can be made. This requires about 8 minutes at the present time.

The oxygen-sensitive dye used (SCCN) was obtained from Frontier Scientific (Logan, UT) and used without further purification. The peak absorption and emission for this dye are near 635 and 694 nm, respectively. We used a 30 mm diameter cylindrical solid phantom (1% Intralipid + 10 mg/liter SCCN + 2% Agar) as the background medium which had $\mu_a = 0.005/\text{mm}$ and $\mu_s' = 1.0/\text{mm}$. A glass tube (10 mm outer diameter, 9.5 mm inner diameter) was inserted as a target at different positions, as shown in Figs. 1a and 1b. The target tube contained a solution with the same amount of mixture of Intralipid and SCCN as the background. Thus both the target and background had the same scattering/absorption coefficients and fluorophore concentration. The lifetime contrast was introduced by varying

#1668 - $15.00 US
Received September 17, 2002; Revised December 18, 2002
(C) 2002 OSA

the amount of oxygen content in the target and background. The gas delivery system, shown in Fig. 1c, was a simple home-made system designed to obtain only three differing oxygen concentrations where the oxygen partial pressure (pO_2) above the target solution was 0, 0.21, and 1.0 atm. Since we found that lowering the oxygen content of the target (0 atm) gave the greatest lifetime contrast with our system, we used 0 atm pO_2 above the target and 1 atm pO_2 above the background for all our experiments. In these experiments, nitrogen was bubbled into the target solution for a half hour while the background was simply open to air. Finally, we conducted an experiment with homogeneous phantom where the target and the background had the same oxygen concentration (1 atm). This experiment was aimed to see if the 0.5 mm thickness of the target tube and the absence of agar in the target have significant effect on our results.

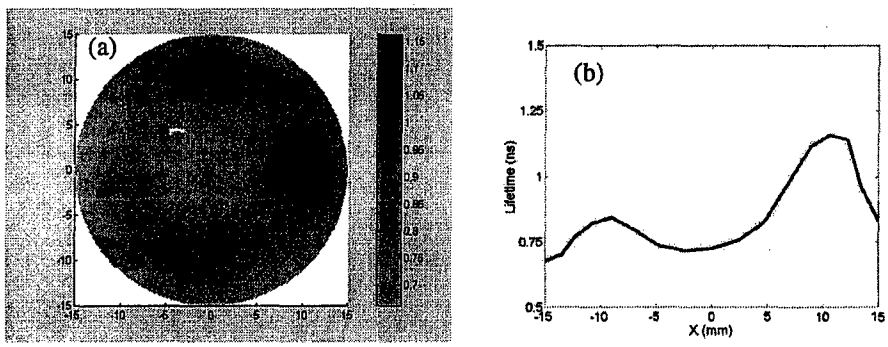

Fig. 2. (a) Reconstructed lifetime image with lowered oxygen content in the target (3 o'clock). The axes (left and bottom) illustrate the spatial scale, in millimeters, whereas the color scale (right) records the fluorescence lifetime, in nanoseconds. (b) Lifetime profile along a horizontal cut line through the centers of both the target and background.

3. Results and Discussion

The finite element mesh used for obtaining the results shown in this section consisted of 249 nodes and 448 triangle elements. The final images reported are the result of 20 iterations. Figure 2a presents the reconstructed lifetime image when the target was positioned at 3 o'clock, while Fig. 2b gives the lifetime profile along a cut-line through the centers of both the target and background as shown in Fig. 1a. As can be seen, the target is clearly detected. We note that the peak lifetime value of the target and the value of the background lifetime are in excellent agreement with the expected values of 1.14 and 0.80 ns for the target and background, respectively (the expected lifetime values of the dye solution at 0 and 1 atm pO_2 were measured using a standard lifetime spectrometer). While the target is accurately located, the target size is underestimated in this case. The lifetime image and its profile for the target at a deeper location (12 o'clock) are shown in Figs. 3a and 3b. While we note that the target is correctly located and that the lifetime values of both the target and background are comparable to the expected values, we see that the overall quality of reconstruction in this case is worse than the image shown in Figs. 2a and 2b. We believe the degradation of image quality in this case is primarily attributed to the lower signal-to-noise ratio (SNR) available when the target is embedded at a larger depth from the boundary. This low SNR case also gives more artifacts around the boundary as we see in Fig. 3a. The recovered lifetime image for the homogeneous case is depicted in Fig. 4 where we can see that the target tube and agar concentration used do not affect our reconstructions significantly.

In summary, we have presented reconstruction of lifetime maps based an oxygen-sensitive dye in turbid media using ac excitation and fluorescent data. We have demonstrated quantitative imaging ability for recovering fluorescence lifetime in centimeter tissue-like phantoms. Thus oxygen concentration maps can be obtained for biomedical diagnosis. It should be pointed out that the reconstruction algorithm presented here is applicable to non-

#1668 - $15.00 US
Received September 17, 2002; Revised December 18, 2002
(C) 2002 OSA

singlet delay of fluorescent dyes for detection of low oxygen concentration contrast [4]. Unlike the fluorescence lifetime imaging (FLIM) reported thus far [19], the lifetime tomography described here is built upon the model-based reconstruction method, thus suitable for imaging large tissues such as breast. This study represents our initial step toward *in vivo* fluorescence lifetime tomography. While the results presented are promising, we realize that improving SNR for FLT remains as a challenge.

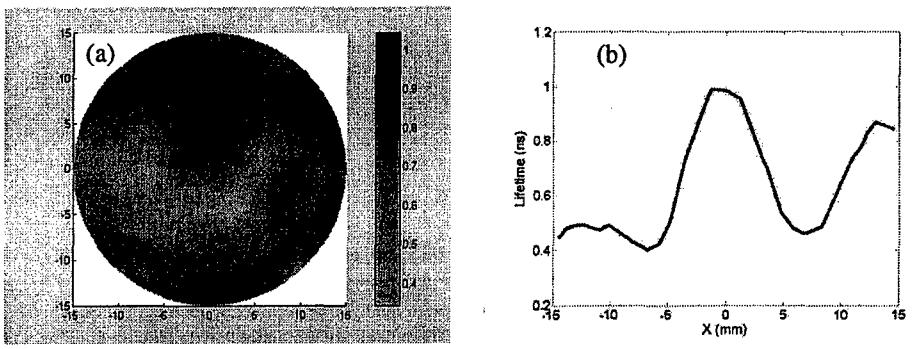

Fig. 3. (a) Reconstructed lifetime image with lowered oxygen content in the target (12 o'clock). The axes (left and bottom) illustrate the spatial scale, in millimeters, whereas the color scale (right) records the fluorescence lifetime, in nanoseconds. (b) Lifetime profile along a horizontal cut line through the center of the target.

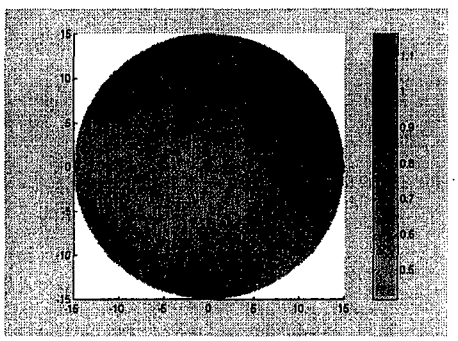

Fig. 4. Reconstructed lifetime image with homogeneous oxygen content in the target and background. The axes (left and bottom) illustrate the spatial scale, in millimeters, whereas the color scale (right) records the fluorescence lifetime, in nanoseconds.

Acknowledgement

This research was supported in part by a grant from the Department of Defense (DOD) (BC 980050).

#1668 - $15.00 US

(C) 2002 OSA

Received September 17, 2002; Revised December 18, 2002